Rock Mechanics and Rock Engineering (2024) 57:7461–7472
https://doi.org/10.1007/s00603-024-03931-5

ORIGINAL PAPER

Controlling Borehole Geometry as a Feasible Strategy for Optimization of Heat Extraction in Geothermal Systems

Dazhao Lu[1] · **Wei Wu**[1]

Received: 22 December 2023 / Accepted: 22 April 2024 / Published online: 10 May 2024

Abstract

Optimizing the heat extraction performance of geothermal systems is a long-standing issue in the study of geothermal energy. Besides the heat extraction in fractured hot rock, minimizing the heat loss during water flowback through boreholes is also critical for the system performance. Here, we conducted a series of experimental and numerical studies to understand the controlling factors of heat extraction rate and efficiency and to explore practical approaches for the optimization of heat extraction performance in a geothermal borehole. We performed water flow experiments to observe the heat extraction from neighboring hot granite and reproduced the heat extraction process using a three-dimensional water flow model. Our results show that the heat extraction rate first increases with a higher flow rate to the maximum value and then decreases with a further rise in flow rate. The heat extraction efficiency decreases constantly with a higher flow rate. To improve the heat extraction performance with both the heat extraction rate and efficiency approaching the maximum values, we scaled up the laboratory-scale borehole and found that the heat extraction performance is enhanced with a triangular zone of heat extraction and a reduced zone of low-temperature water along a field-scale borehole. We finally discovered that a proper control of borehole geometry, such as section diameters along a multi-section borehole and bending angle of borehole trajectory, is a feasible strategy to modulate the heat extraction performance in a geothermal borehole and to replenish the heat loss during water flowback.

Highlights

- Experimental and numerical studies are conducted to understand the controlling factors of heat extraction rate and efficiency.
- Heat extraction performance is enhanced with a triangular zone of heat extraction and a reduced zone of low-temperature water.
- Multi-section borehole is a feasible strategy to modulate the heat extraction performance in a geothermal borehole.
- Proper bending angle of borehole trajectory is another feasible strategy to optimize the heat extraction performance.

Keywords Geothermal energy · Heat extraction · Flow rate · Multi-section borehole · Borehole trajectory

1 Introduction

Geothermal energy is the almost inexhaustible heat from the earth's interior and has substantial potential as a clean energy to reduce global carbon emissions (Barbier 2002; Li et al. 2022). The heat extraction performance of geothermal systems relies primarily on the thermal properties of host rock (e.g., heat-producing granite) and the physical characteristics and operational parameters of working fluid (e.g., water and carbon dioxide). Extensive efforts have been

✉ Wei Wu
wu.wei@ntu.edu.sg

[1] School of Civil and Environmental Engineering, Nanyang Technological University, Singapore, Singapore

made to improve the heat extraction performance, such as enhanced geothermal systems to create hydraulically fractured reservoirs (Li et al. 2021; Rathnaweera et al. 2020), advanced drilling technologies to access deeper and hotter geothermal sources (Ji et al. 2021; Rossi et al. 2020), and novel exchanger designs to enable better heat transfer and energy conversion (Hu et al. 2022; Liu et al. 2022). These efforts aim essentially to improve the amount of heat energy transferred to working fluid and to reduce the loss of heat energy due to the frictional, gravitational, and Joule–Thomson effects (Phuoc et al. 2019; Zhang et al. 2022), which are commonly known as heat extraction rate and efficiency, respectively.

Maximizing the heat extraction rate and efficiency is an ideal scenario to optimize the heat extraction performance of geothermal systems. Numerous studies have demonstrated dissimilar variations of heat extraction rate and efficiency under geological (e.g., heat distribution and conduction) and operational (e.g., flow rate and injection pressure) conditions. The heat extraction rate can be improved by appropriate coupling of thermo–hydro–mechanical processes (Pandey and Vishal 2017; Sun et al. 2021), efficient fluid flow and heat flow in fracture networks (Chen and Zhao 2020; Xu et al. 2023), and low-salinity working fluid (Borgia et al. 2012), but cannot be increased constantly with a higher flow rate (Zhao et al. 2022). The heat extraction efficiency has different quantitative indicators, showing diverse relationships with the geological and operational conditions. For instance, the energy efficiency defined as the ratio of produced thermal energy to consumed internal energy is correlated positively with fracture permeability and rock thermal conductivity and negatively with flow rate (Zeng et al. 2013). The heat extraction efficiency defined as the ratio of average outlet temperature to heat recovery factor increases with a higher injection pressure until reaching a specified limit (Sun et al. 2020). The heat extraction efficiency is also defined as the ratio of pump energy consumption rate to energy extraction rate and inversely proportional to in-situ stress (Shu et al. 2022). Hence, the heat extraction rate and efficiency assessed by various geological and operational factors can be complex and may vary in different manners. In engineering practice, the heat extraction rate and efficiency are critical for the thermal power output and the heat recovery effectiveness of geothermal systems, respectively (Li et al. 2023). However, how to optimize the heat extraction performance remains a topic of debate, and what factors controlling the variations of heat extraction rate and efficiency are still unclear.

The objectives of this study include understanding the controlling factors of heat extraction rate and efficiency according to the experimental and numerical studies and exploring practical approaches to improve the field-scale heat extraction performance based on the laboratory-scale fundamental studies. The study sheds light on the heat extraction while water flowing through the borehole. Meanwhile, the loss of geothermal heat extracted from fractured hot rock can be minimized and replenished during water flowback. We first conducted three suits of water flow experiments to observe the variation of water temperature in a laboratory-scale borehole under different combinations of surrounding temperature and flow rate. We then built a three-dimensional (3D) water flow model using COMSOL Multiphysics software to reproduce the experimental process and to evaluate the heat extraction rate and efficiency. We adopted simple and common definitions of heat extraction rate and efficiency, which are the heat energy extracted by water per unit time and in relative to the heat energy removed from rock, respectively. We finally extended the numerical model from laboratory scale to field scale and discussed a feasible strategy by changing borehole geometry to improve the heat extraction performance of a geothermal borehole.

2 Methods

2.1 Experimental Method

We performed a series of water flow experiments through a drilled borehole to extract heat from surrounding hot rocks. Bukit Timah granite sourced from central Singapore was used as the rock medium. The medium-grained granite was composed of 62% feldspar, 32% quartz, 5% black mica, and 1% hornblende. The bulk density, porosity, Young's modulus, and intrinsic permeability of the granite were 2660 kg/m^3, 0.26%, 74 GPa, and 1.3 μD, respectively. The thermal conductivity, specific heat capacity, and thermal expansion coefficient of the granite were 3.5 W/(m K), 800 J/(kg K), and 7×10^{-6} K^{-1}, respectively. A granite core with a diameter of 50 mm was cut into two cylindrical specimens with a length of 100 mm using a diamond saw, and the specimen ends were ground within 0.02 mm flatness using sandpaper. A small borehole with a diameter of 6 mm was drilled along the specimen axis to facilitate water flow and heat extraction.

In the experimental setup, the drilled specimen was placed between two iron coreholders with internal waterpipes. Two fiberglass sheets were inserted between the specimen and the coreholders to minimize heat loss from the specimen ends. The specimen was sealed using a shrinkable plastic tube and fixed on the coreholders using a steel wire. The side wall of the sealed specimen was covered by a mica heater, which is capable of heating up to 250 °C and controlled by a closed-loop temperature controller with temperature fluctuation less than 1 °C. A Vindum pump was utilized to provide a continuous flow of distilled water and to monitor flow rate and water pressure. Five thermocouples were used to measure water and granite temperatures: three thermocouples (A, B, and S) attached on the upper end of the specimen, the wall of the borehole, and the side wall of the specimen to monitor the temperature distribution over the cross-sectional area of the specimen, and two thermocouples (C and D) placed near the borehole ends to record the inflow and outflow temperatures of distilled water (Fig. 1). The thermocouples with a measurement accuracy of ± 1.5 °C were connected to a LabVIEW data acquisition system at a sampling rate of 10 Hz. An axial load of 1 kN was applied to fix the setup, and the room temperature was 22 °C.

We conducted three suites of water flow experiments to investigate the heat extraction performance using distilled water at three flow rates (5, 10, and 15 ml/min) through the heated specimen at three surrounding temperatures of 80, 100, and 120 °C (Fig. 2). The inflow and outflow water pressures were 0.6 MPa and atmospheric, respectively. The experimental procedure included three sequential and three reverse-sequential steps. For the three sequential steps, the specimen was first heated to a desired temperature, and distilled water was pumped into the borehole at a constant flow rate of 5 ml/min. The flow rate was kept for about 30 min to ensure the inflow and outflow temperatures stable. The flow rate was subsequently increased to 10 and 15 ml/min and kept for similar durations. After a 30-min break, the specimen temperature was recovered to the desired temperature. In the three reverse-sequential steps, distilled water was first pumped into the borehole at a constant flow rate of 15 ml/min for about 30 min, followed by pumping with flow rates of 10 and 5 ml/min and maintained for similar durations. The axial load, surrounding temperature, and flow rate were fixed during the experiments, and the inflow and outflow temperatures were recorded by the data acquisition system.

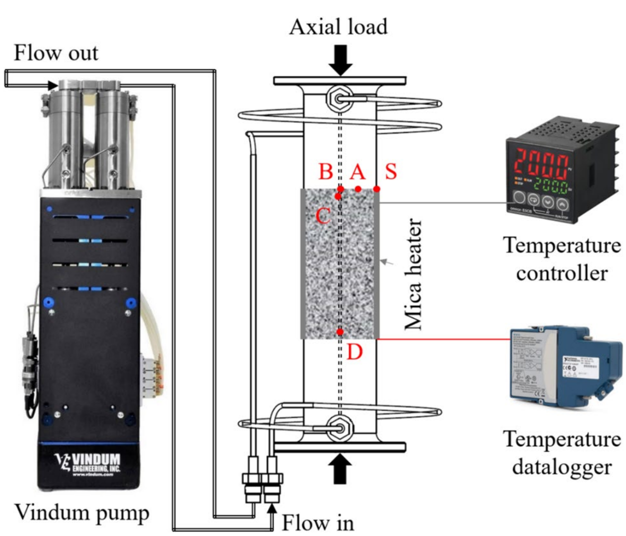

Fig. 1 Schematic diagram of water flow experimental setup. Red dots indicate the locations of thermocouples

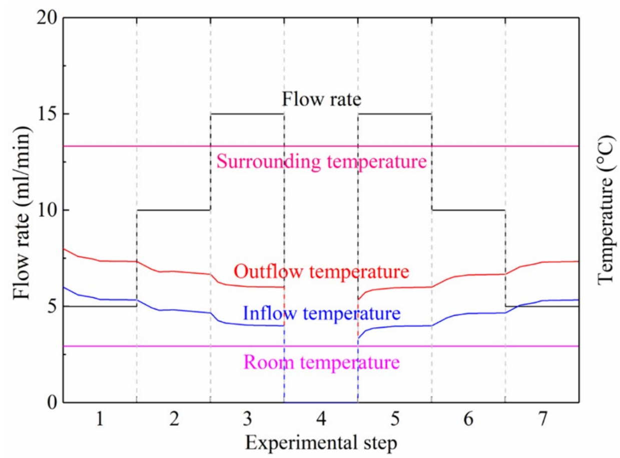

Fig. 2 Experimental procedure of water flow experiment. The surrounding temperatures used are 80, 100, and 120 ºC. The inflow and outflow temperatures (not to scale) vary depending on the surrounding temperature and flow rate

2.2 Numerical Method

We built a 3D water flow model using COMSOL Multiphysics software to reproduce the heat extraction process. We assumed that the granite matrix was homogeneous, incompressible, and impermeable. Water flow was laminar within the borehole. The temperature distribution in water and granite was solved under a steady-state condition. The water flow model, as shown in Fig. 3a, has the same dimension as the granite specimen used in the water flow experiment. The

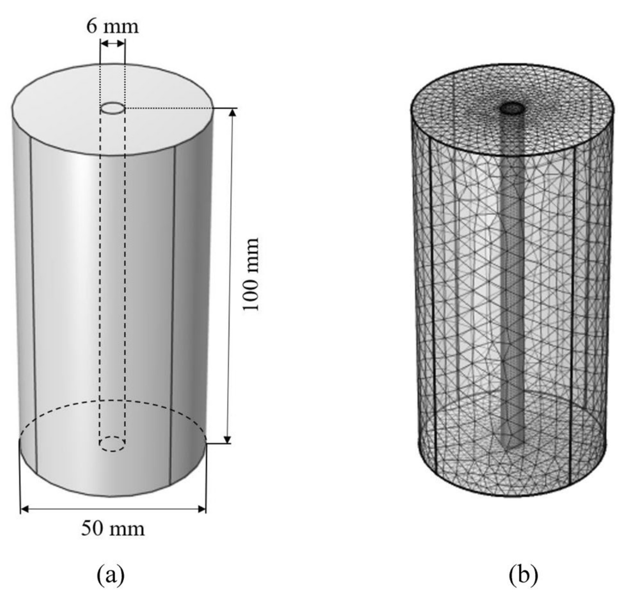

Fig. 3 Laboratory-scale water flow model, including **a** model geometry and **b** model mesh

model was meshed with tetrahedral and hexahedral elements and with finer elements in and around the borehole (Fig. 3b).

In the model setup, the equations of energy conservation for water and rock were expressed according to the heat transfer equation (Jäckel et al. 2019):

$$\rho_w C_{pw} \frac{\partial T}{\partial t} + \rho_w C_{pw} \mathbf{u} \cdot \nabla T = -\nabla \cdot \left(k_w \nabla T\right) + Q \tag{1}$$

$$\rho_r C_{pr} \frac{\partial T}{\partial t} = -\nabla \cdot \left(k_r \nabla T\right) + Q \tag{2}$$

where ρ_w and ρ_r [kg/m^3] are the densities of water and rock, respectively, C_{pw} and C_{pr} [J/(kg·K)] are the specific heat capacities of water and rock, respectively, T [K] is the time-dependent temperature field, t [s] is the elapsed time, $\mathbf{u}$ [m/s] is the flow velocity vector of water, k_w and k_r [W/(m K)] are the thermal conductivities of water and rock, respectively, and Q [J] is the other forms of energy in the domain, including the viscous dissipation heating, the Joule heating, and the pressure work.

The momentum conservation is written according to the Navier–Stokes equation (Tritton 1977):

$$\rho_w \frac{\partial \mathbf{u}}{\partial t} + \rho_w(\mathbf{u} \cdot \nabla \mathbf{u}) = -\nabla p + \mu \nabla^2 \mathbf{u} + \mathbf{F} \tag{3}$$

where p [Pa] is the water pressure, μ [kg/(m s)] is the kinematic viscosity of water, and $\mathbf{F}$ [N/m^3] is the body force vector due to the gravity of water.

The continuity equation of mass conservation is (Tritton 1977):

$$\frac{\partial \rho_w}{\partial t} + \nabla \cdot \left(\rho_w \mathbf{u}\right) = 0 \tag{4}$$

For the boundary conditions, the upper and lower ends of the granite specimen were thermally insulated, and the temperature on the side wall was fixed between 60 and 200 °C. The water inflow velocity was associated with the flow rate in a range of 1–20 ml/min. The inflow temperature was set as the room temperature (22 °C) to eliminate the influence of uncontrollable inflow temperature in the experimental study and to focus on the heat exchange at the rock–water interface. Following the experimental procedure, the inflow and outflow pressures of water were 0.6 MPa and atmospheric, respectively.

3 Results

3.1 Experimental Results

The experimental results demonstrate changes in water and granite temperatures during the heat extraction process. As shown in Fig. 4a, taking 100 °C surrounding temperature as an example, the temperatures measured by the thermocouples A and S show that the granite temperature on the upper end of the specimen keeps roughly constant during the experiment, while the granite temperature on the inner wall of the borehole measured by the thermocouple B is reduced during the sequential and reverse-sequential steps and recovered between these steps. The sequential and reverse-sequential steps thus start on the same thermal condition, allowing us to compare the differences between the inflow and outflow temperatures in these steps. The granite temperatures obtained by averaging the data points in the sequential and reverse-sequential steps indicate the temperature reduction from the inner wall of the borehole to the side wall of the specimen (Fig. 4b). At different surrounding temperatures (i.e., 80, 100, and 120 °C), the temperature reductions of neighboring granite around the borehole are similar (e.g., between the thermocouples A and B). A higher surrounding temperature exhibits a larger temperature reduction near the side wall of the specimen (e.g., between the thermocouples A and S), implying that more heat is extracted by flowing

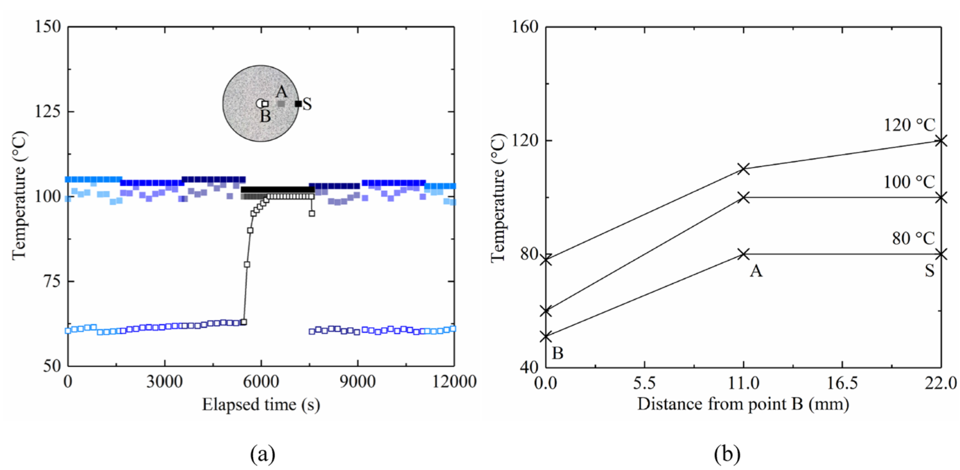

Fig. 4 **a** Temperature recovery between sequential and reverse-sequential steps at 100 °C surrounding temperature; the inset shows the specimen end with the locations of three thermocouples, and **b** temperature reductions from thermocouple S at 80, 100, and 120 °C surrounding temperatures to thermocouples A and B

water. In addition, the water temperatures measured by the thermocouple B are below 100 °C in these cases, indicating that water remains in the liquid phase.

The water temperatures at the lower and upper ends of the borehole are described as inflow and outflow temperatures, respectively. Figure 5 shows that the outflow temperature higher than the inflow temperature demonstrates successful heat extraction from the heated granite. In the three suites of water flow experiments, both the inflow and outflow temperatures increase with a higher surrounding temperature and decrease with a higher flow rate. Both the inflow and outflow temperatures are relatively stable at a low surrounding temperature and become fluctuating at a high surrounding temperature. A high flow rate enhances the temperature fluctuation owing to a large variation of water temperature along the borehole. The inflow and outflow temperatures are slightly different in the sequential and reverse-sequential steps likely due to different amounts of available heat after previous steps.

3.2 Numerical Results

Figure 6 presents the validation of the numerical model by comparing the temperature differences obtained from the experimental and numerical studies. The experimental temperature difference is calculated based on the average inflow and outflow temperatures in the sequential and reverse-sequential steps. The error bar is plotted based on the standard error. The numerical temperature difference is obtained based on the fixed inflow temperature and the

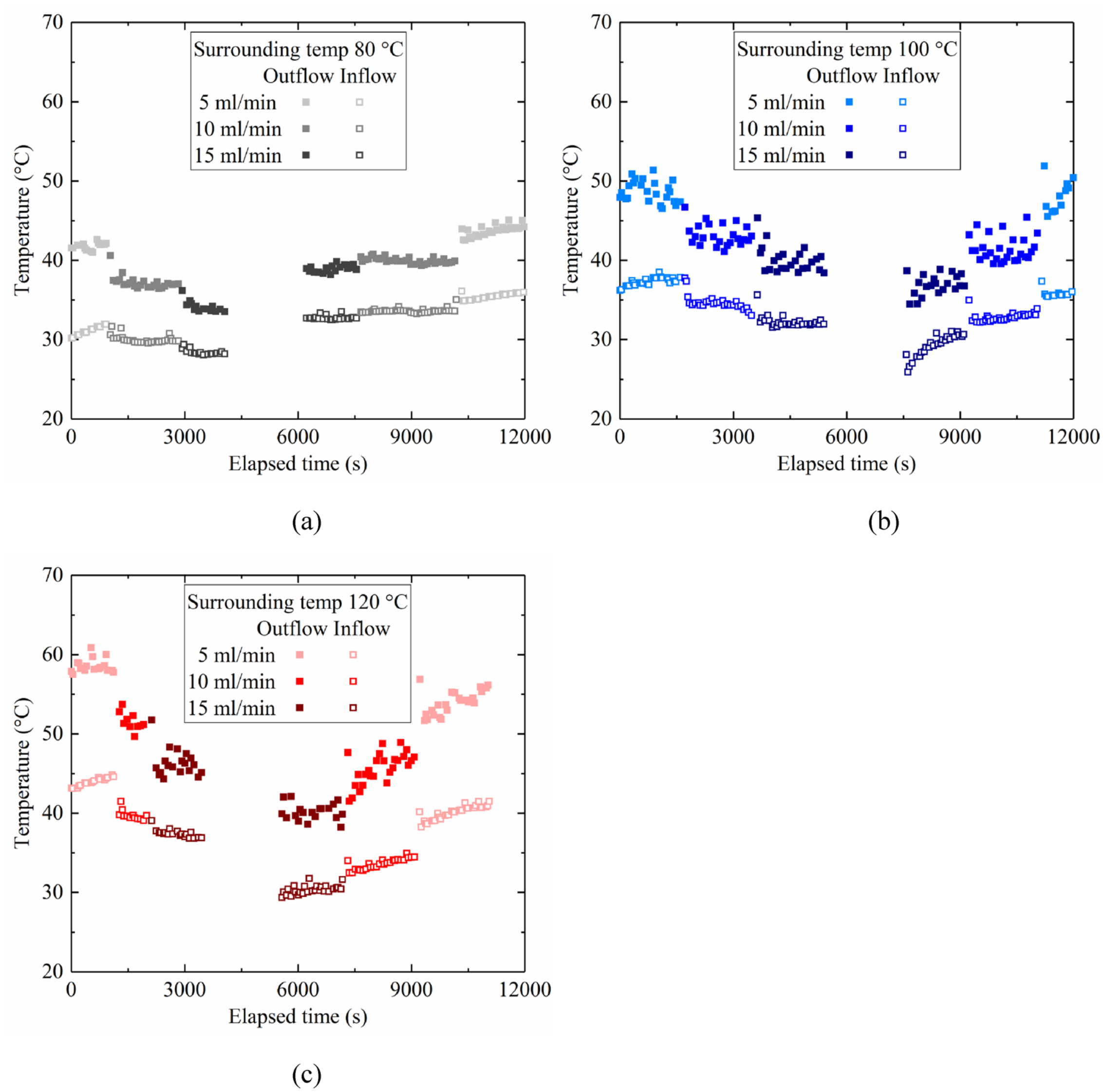

Fig. 5 Inflow and outflow temperatures during water flow experiments with 5, 10, and 15 ml/min flow rates at **a** 80, **b** 100, and **c** 120 °C surrounding temperatures

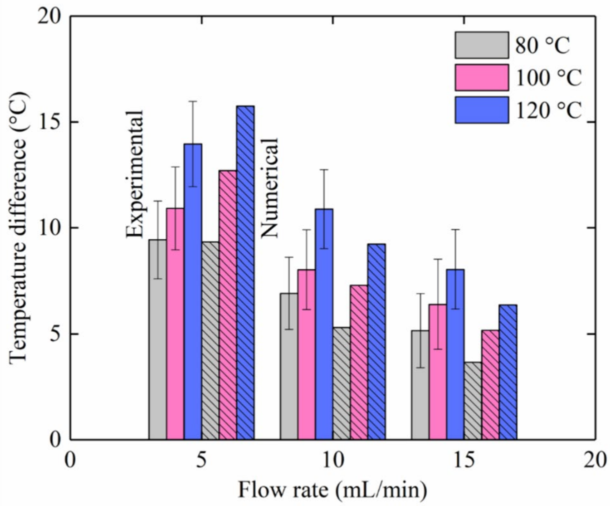

Fig. 6 Temperature difference of inflow and outflow temperatures between experimental (non-shadowed) and numerical (shadowed) results of water flow experiments with 5, 10, and 15 ml/min flow rates at 80, 100, and 120 °C surrounding temperatures

average outflow temperature. For the three surrounding temperatures, the temperature differences at different flow rates from the numerical study are close to the experimental results and fall in the range of error bar. However, measuring the temperature differences is insufficient to evaluate the heat extraction performance from the heated granite.

The heat extraction process is associated with heat conduction in rock, heat advection in water, and heat convection at the rock–water interface (Pandey et al. 2018). To quantify these characteristics involved in this process, we used the specific enthalpy change of water Δh [kJ/kg], the temperature loss of rock D, as well as the heat extraction rate P [W] and efficiency γ of rock–water interface, as follows:

$$\Delta h = C_{pw}(T_{\text{out}} - T_{\text{in}}) \tag{5}$$

$$D = \frac{T_{r0} - T_{rt}}{T_{r0}} \times 100\% \tag{6}$$

$$P = C_{pw}\rho_w q(T_{\text{out}} - T_{\text{in}}) \tag{7}$$

$$\gamma = \frac{T_{\text{out}} - T_{\text{in}}}{T_{r0} - T_{\text{in}}} \times 100\% \tag{8}$$

where T_{out} [K] and T_{in} [K] are the outflow and inflow temperatures, respectively, T_{r0} and T_{rt} [K] are the initial temperature of rock and the final temperature at equilibrium, respectively, Δt is the unit time, and q [m^3/s] is the volumetric flow rate of water.

As shown in Fig. 7, a change in specific enthalpy of water reflects the variations of internal energy and flow work (Wang et al. 2017) and increases with a higher surrounding temperature and a lower flow rate. A larger difference of inflow and outflow temperatures amplifies the specific enthalpy change. A temperature loss of rock is resulted from the heat exchange at the rock–water interface and should not exceed 10% for sustainable heat extraction (Lei et al. 2020). A higher surrounding temperature and a larger flow rate lead to a greater rock temperature loss. A higher surrounding temperature causes increases in heat extraction rate and efficiency, which is consistent with the numerical results of full-scale geothermal systems (Sun et al. 2020; Huang et al. 2023). A larger flow rate induces a decrease in heat extraction efficiency. However, the heat extraction rate first increases to the maximum value and then decreases with a further rise in flow rate. The reduction of heat extraction rate at a very high flow rate is unexpected, and similar results can be observed based on the net power of Davis and Michaelides (2009) and the Carnot cycle power of Harris et al. (2021). The physical mechanism behind the reduction of heat extraction rate is likely associated with multiple geological and operational factors involved in the heat extraction process but remains largely unconstrained.

4 Discussion

Our results highlight different variations of heat extraction rate and efficiency as functions of surrounding temperature and flow rate. To optimize the heat extraction performance of geothermal systems, it is essential to understand the controlling factors for the variations of heat extraction rate and efficiency. Toward this end, a laboratory-scale borehole is insufficient to accommodate the fully heat extraction process, given the long heat exchange duration (Fig. 5) and a desired high flow rate (Gan and Elsworth 2016). Hence, we scaled up the numerical model by increasing specimen diameter, specimen length, and borehole diameter proportionally to 2.5, 5, and 0.3 m, respectively. We then piled up the amplified models to form a field-scale borehole with a length of 100 m (Fig. 8a). We considered a surrounding temperature of 150 °C and investigated the effect of flow rate (0.02–10 l/s) on the heat extraction process. The inflow temperature and pressure of water remained 22 °C and 0.6 MPa, respectively, and the outflow pressure was atmospheric. Note that the field-scale borehole represents a section of geothermal borehole with effective heat extraction, not a full-length borehole in geothermal systems.

The results of field-scale water flow modeling, as shown in Fig. 9, exhibit the temperature distribution in water and rock below and above the dashed line, respectively, covering the zoom-in region in Fig. 8b. The distance from the

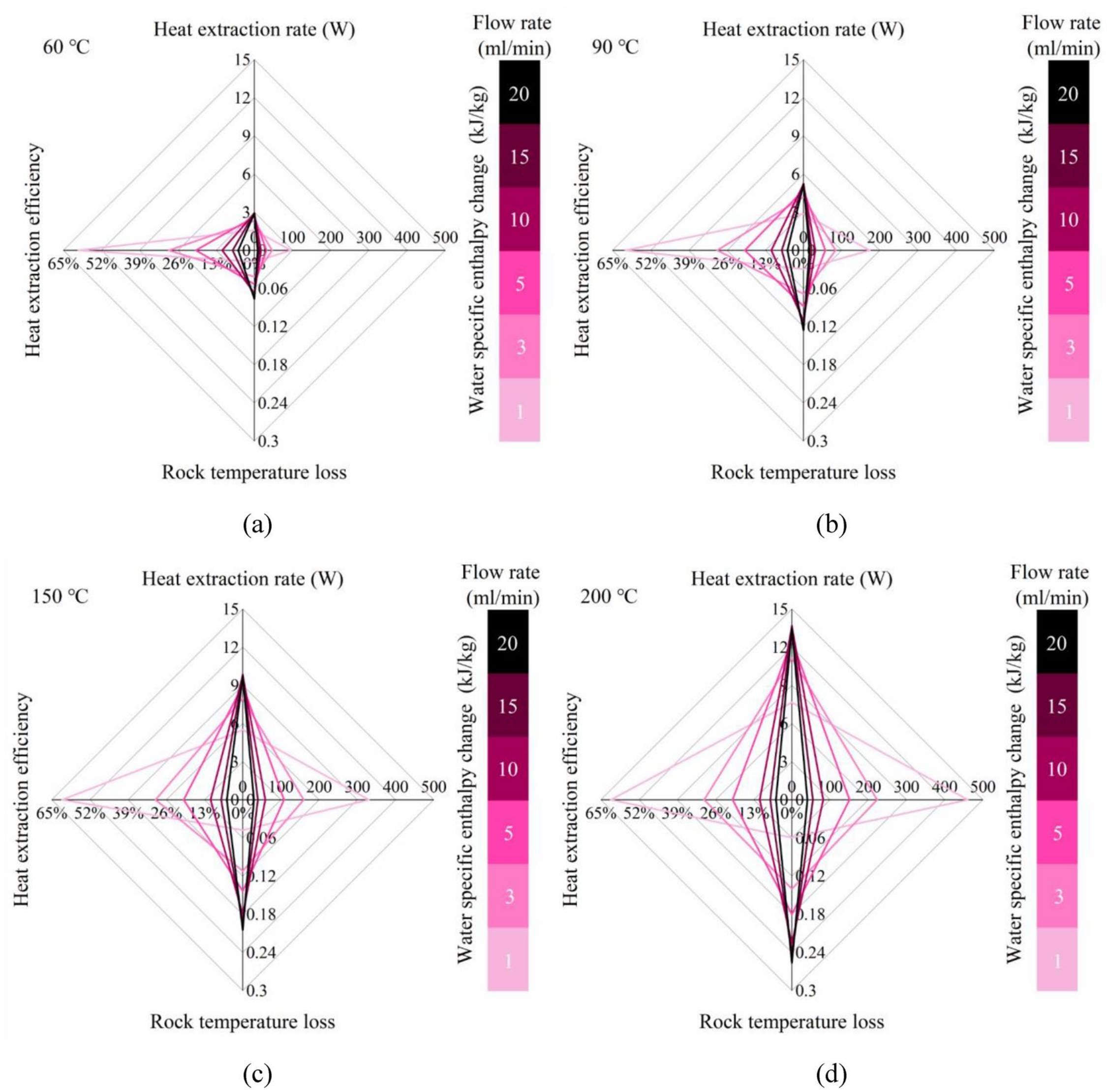

Fig. 7 Heat extraction characteristics, including water-specific enthalpy change, rock temperature loss, as well as heat extraction rate and efficiency, as a function of flow rate at surrounding temperatures of **a** 60, **b** 90, **c** 150, and **d** 200 °C

borehole axis is normalized by the model radius (1.25 m). After reaching temperature equilibrium in the model, both the temperatures of water and rock increase nonlinearly with a higher flow rate. The water temperature near the inflow port rises slightly, indicating an unfavorable scenario for heat exchange (Mohammed 2009). The water temperature beyond the inflow port distributes uniformly in the radial direction of the borehole, a favorable scenario for heat exchange, and increases notably in the longitudinal direction. The reduction of rock temperature initiates near the inflow port and expands parallel and perpendicular to the borehole axis to form a heat exchange zone. With increasing flow rate, the shape of heat exchange zone changes from a triangle to a trapezoid. The triangular zone was also observed in previous studies (Gao and Shi 2021; Kang et al. 2022). Our results reveal that the size and shape of heat exchange zone are related to the flow rate. At a low flow rate, a small size of triangular zone indicates that the effective heat exchange is limited near the inflow port and the available heat around the 100 m borehole is largely unextracted (Fig. 9a and b). At a high flow rate, the heat exchange zone is extended into a trapezoidal shape, resulting in an insufficient heating of flowing water (Fig. 9e and f). Therefore, the heat extraction rate can be optimized at an intermediate flow rate when the maximum size of triangular zone is achieved (Fig. 9c and d). Meanwhile, the heat extraction efficiency decreases with a higher flow rate as indicated by an increasing size of low-temperature area (as indicated by the blue color) in the borehole, showing that the variation of heat extraction

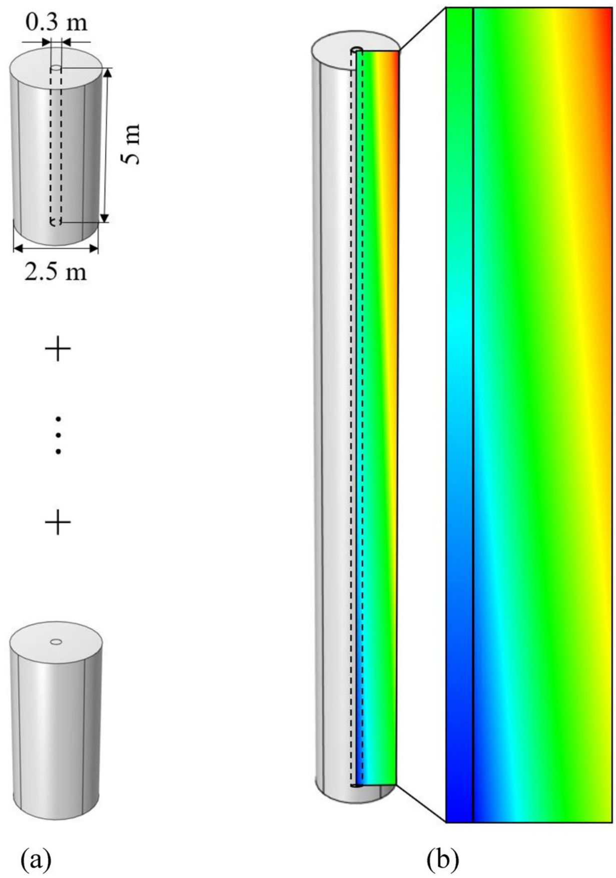

Fig. 8 Field-scale water flow model, including **a** building up this model using laboratory-scale models and **b** highlighting temperature distribution in water and granite using color section

efficiency with increasing flow rate is different from that of heat extraction rate.

The maximum values of heat extraction rate and efficiency appear at different flow rates (Fig. 9a and d), indicating that the heat energy extracted by water per unit time and in relative to the total energy from rock cannot achieve the maximum values at the same time. A compromise solution for the improvement of heat extraction performance is to make the heat extraction rate approach the maximum value and to keep the heat extraction efficiency as high as possible at the corresponding flow rate. However, for a large difference of flow rates related to the maximum values of heat extraction rate and efficiency (e.g., 50 times in Fig. 9a and d), controlling flow rate may not lead to a satisfactory compromise solution in a geothermal borehole.

To address this challenge, we were inspired by section drilling, which means borehole drilling with multiple sections in a stepping-down mode (Hosein et al. 2019; Talalay and Hong 2021). Controlling the diameters of borehole sections can be an effective strategy to improve the heat extraction performance. For a single-section borehole with a diameter of 0.3 m and a length of 100 m, flowing water at a fixed rate of 1 l/s causes a trapezoidal zone (Fig. 10a), indicating insufficient water heating. We modified the borehole with five sections each with a length of 20 m and a diameter changing from 0.5 on the top to 0.3 m on the bottom with an interval of 0.05 m. Under the same geological and operational conditions (Fig. 9), the heat exchange zone over the multi-section borehole becomes a triangular zone (Fig. 10b), meaning the improvement of heat extraction rate. The size of low-temperature area in the multi-section borehole representing ineffective heat extraction is much smaller than that in the single-section borehole, showing the improvement of heat extraction efficiency. Controlling the diameters of borehole sections is thus proved as an effective strategy. Although the borehole diameters are determined by drill bits, the lengths of multiple sections can be controlled in the borehole design.

Another strategy of controlling borehole geometry to improve the heat extraction performance is changing the borehole trajectory, which was inspired by the heat transfer in ground heat exchangers using inclined boreholes (Cui et al. 2006; Marcotte and Pasquier 2009). We considered a single-section borehole with a diameter of 0.3 m and a length of 100 m containing flowing water at a fixed rate of 1 l/s. As shown in Fig. 11, we locked the upper half of the borehole vertically and bent the lower half from a sub-vertical angle (15°) to a horizontal angle (90°). The two halves were connected by a short arc section with a radius of 1.5 m, which was insignificant to affect the heat extraction performance. The results show that the heat exchange zone along the borehole expands in a triangle zone when the lower half deviates from 15° to 30° and becomes a trapezoidal zone at 45°. The heat exchange zone reduces to a triangle zone at 60° and shrinks until 90°. The variation of heat exchange zone indicates that a bending angle in a range of 30–60° is suitable to promote the heat extraction performance along the borehole. For a bending angle close to 45°, the formation of triangle zone can be obtained by reducing flow rate (Fig. 9) and by changing borehole diameter (Fig. 10). Our study suggests that borehole geometry, including borehole trajectory and cross-section area, can be controlled to enhance the heat extraction in a geothermal borehole.

5 Conclusions

This study reports a series of experimental and numerical studies to understand the controlling factors of heat extraction rate and efficiency and to explore practical approaches for the improvement of heat extraction performance in a geothermal borehole. Our results show dissimilar variations of heat extraction rate and efficiency as a function of flow rate. In this case, a simple compromise solution with

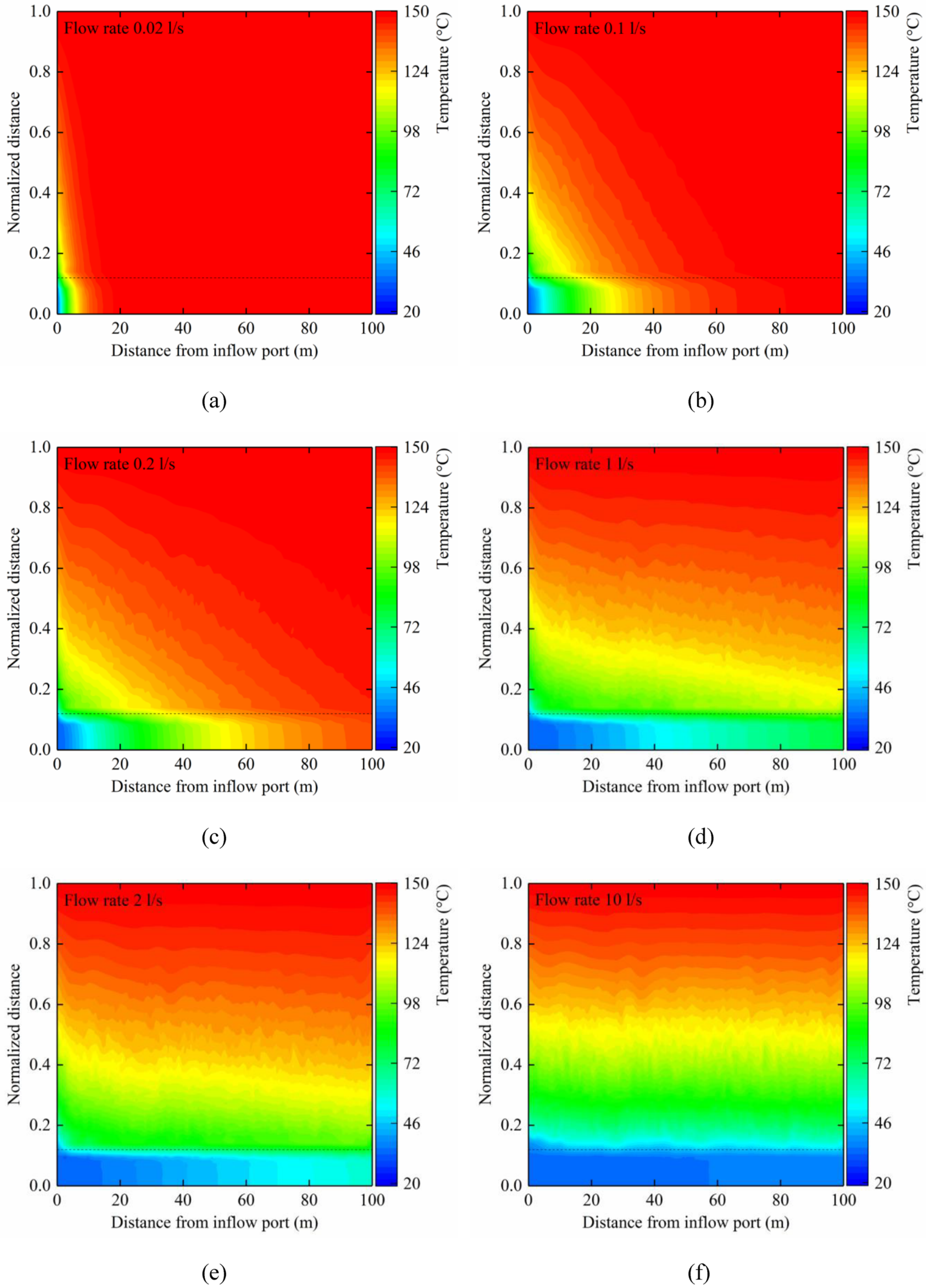

Fig. 9 At a surrounding temperature of 150 °C, temperature distribution of water and rock (below and above the dashed line) as a function of flow rate. The vertical axis is normalized by the model radius

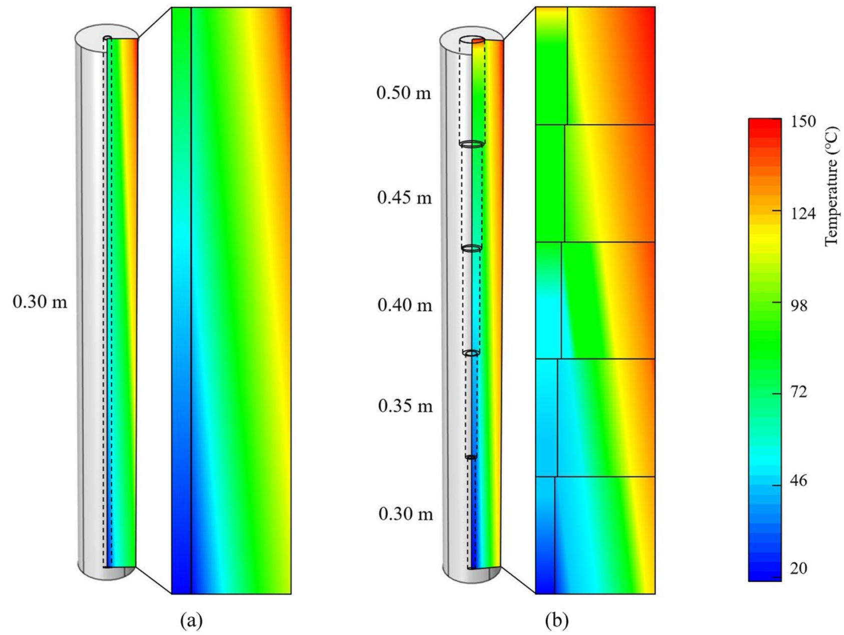

Fig. 10 Temperature distribution in water and rock over **a** a single-section borehole and **b** a multi-section borehole. The number on the left side indicates the borehole diameter

the heat extraction rate approaching the maximum value and the heat extraction efficiency kept as high as possible at the corresponding flow rate may not be feasible, particularly for the case with a large difference of flow rates related to the maximum values of heat extraction rate and efficiency. The study proposes and verifies the modification of borehole geometry to modulate the heat extraction performance in a geothermal borehole. Proper controls of section diameters along a multi-section borehole and bending angle of borehole trajectory can produce a triangular zone of heat extraction and a reduced zone of low-temperature water along the borehole, which are key findings to ensure the optimization of heat extraction performance. These findings can be considered in the design of geothermal systems to minimize the heat loss during water flowback. The study also inspires us to jointly consider other geological and operational factors (e.g., fracture network and fluid viscosity) to further improve the heat extraction performance of geothermal systems.

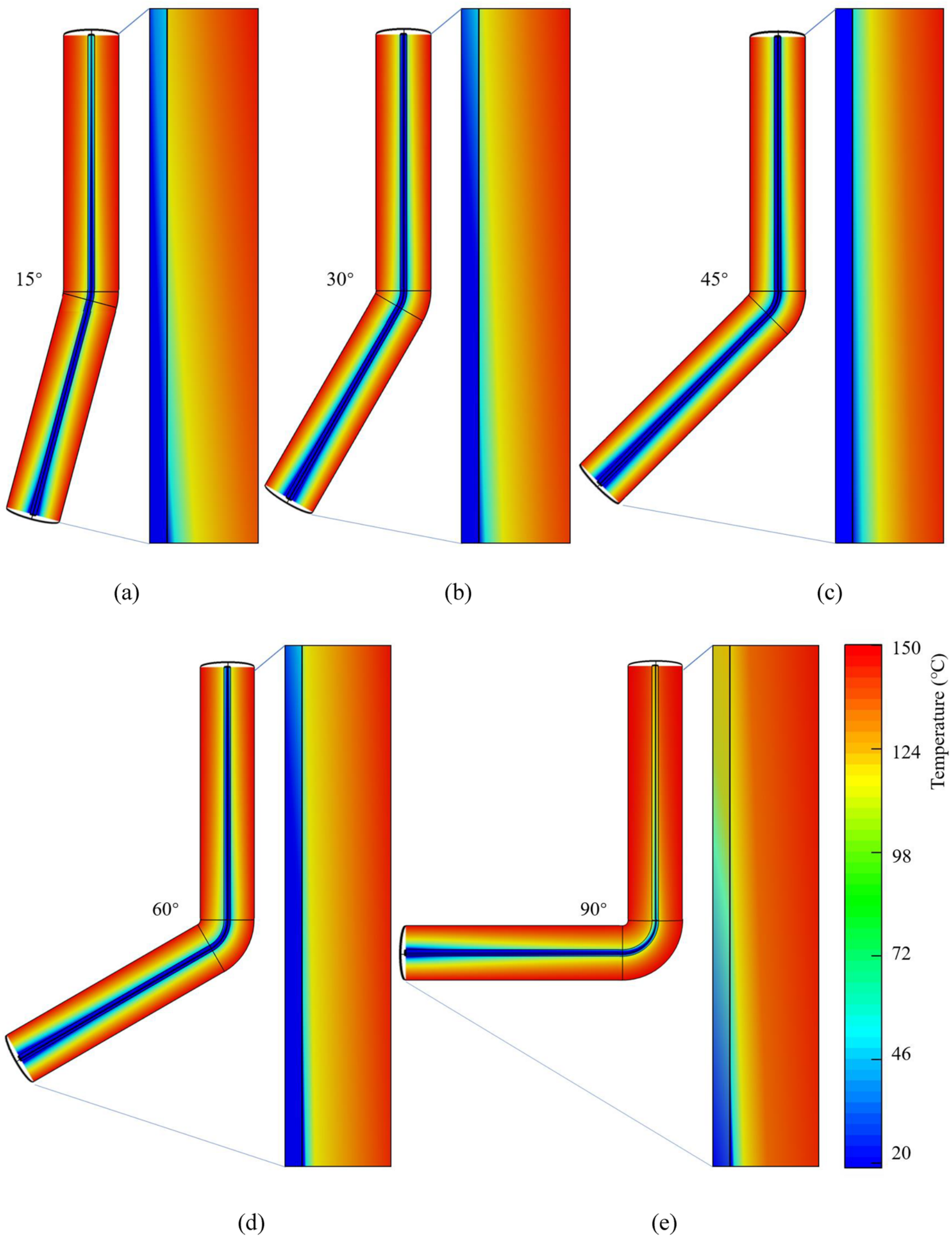

Fig. 11 Temperature distribution along different borehole trajectories with bending angles **a** 15°, **b** 30°, **c** 45°, **d** 60°, and **e** 90°

Acknowledgements This research is supported by the National Research Foundation, Singapore, under its Intra-CREATE Thematic Grant (Award No. NRF2019-THE001-0002).

Funding Funding was provided by National Research Foundation Singapore (Grant number: NRF2019-THE001-0002).

Data availability Data is available upon request.

Declarations

Conflict of interest The authors declare no conflict of interest.

References

Barbier E (2002) Geothermal energy technology and current status: an overview. Renew Sustain Energy Rev 6:3–65

Borgia A, Pruess K, Kneafsey TJ, Oldenburg CM, Pan L (2012) Numerical simulation of salt precipitation in the fractures of a CO_2-enhanced geothermal system. Geothermics 44:13–22

Chen Y, Zhao Z (2020) Heat transfer in a 3D rough rock fracture with heterogenous apertures. Int J Rock Mech Min Sci 134:104445

Cui P, Yang H, Fang Z (2006) Heat transfer analysis of ground heat exchangers with inclined boreholes. Appl Therm Eng 26:1169–1175

Davis AP, Michaelides EE (2009) Geothermal power production from abandoned oil wells. Energy 34:866–872

Gan Q, Elsworth D (2016) Production optimization in fractured geothermal reservoirs by coupled discrete fracture network modeling. Geothermics 62:131–142

Gao J, Shi Q (2021) A new mathematical modeling approach for thermal exploration efficiency under different geothermal well layout conditions. Sci Rep 11:22930
Harris BE, Lightstone MF, Reitsma S (2021) A numerical investigation into the use of directionally drilled wells for the extraction of geothermal energy from abandoned oil and gas wells. Geothermics 90:101994
Hosein R, Serrattan S, Jupiter A (2019) The viability of slim-hole drilling onshore Trinidad. J Pet Explor Prod Technol 9:1307–1322
Hu J, Xie H, Gao M, Li C, Sun Q (2022) Damage mechanism and heat transfer characteristics of limestone after thermal shock cycle treatments based on geothermal development. Int J Rock Mech Min Sci 160:105269
Huang Y, Kong Y, Cheng Y, Zhu C, Zhang J, Wang J (2023) Evaluating the long-term sustainability of geothermal energy utilization from deep coal mines. Geothermics 107:102584
Jäckel R, Gutiérrez Urueta GL, Tapia Rodríguez F, Monreal Jiménez C (2019) Numerical and experimental characterisation of an aeronautic Pitot probe. Aeronaut J 123:890–891
Ji Y, Wang L, Zheng Y, Wu W (2021) Temperature-dependent abrasivity of Bukit Timah granite and implications for drill bit wear in thermo-mechanical drilling. Acta Geotech 16:885–893
Kang F, Li Y, Tang C, Huang X, Li T (2022) Competition between cooling contraction and fluid overpressure on aperture evolution in a geothermal system. Renew Energy 186:704–716
Lei Z, Zhang Y, Zhang S, Fu L, Hu Z, Yu Z, Li L, Zhou J (2020) Electricity generation from a three-horizontal-well enhanced geothermal system in the Qiabuqia geothermal field, China: slickwater fracturing treatments for different reservoir scenarios. Renew Energy 145:65–83
Li T, Tang C, Rutqvist J, Hu M (2021) TOUGH-RFPA: Coupled thermal-hydraulic-mechanical Rock Failure Process Analysis with application to deep geothermal wells. Int J Rock Mech Min Sci 142:104726
Li G, Ji J, Song X, Shi Y, Li S, Song Z, Song G, Xu F (2022) Research advances in multi-field coupling model for geothermal reservoir heat extraction. Energy Rev 1:100009
Li X, Li C, Gong W, Zhang Y, Wang J (2023) Probabilistic analysis of heat extraction performance in enhanced geothermal system based on a DFN-based modeling scheme. Energy 263:125674
Liu G, Zhao Z, Xu H, Zhang J, Kong X, Yuan L (2022) A robust assessment method of recoverable geothermal energy considering optimal development parameters. Renew Energy 201:426–440
Marcotte D, Pasquier P (2009) The effect of borehole inclination on fluid and ground temperature for GLHE systems. Geothermics 38:392–398
Mohammed HA (2009) The effect of different inlet geometries on laminar flow combined convection heat transfer inside a horizontal circular pipe. Appl Therm Eng 29:581–590
Pandey SN, Vishal V (2017) Sensitivity analysis of coupled processes and parameters on the performance of enhanced geothermal systems. Sci Rep 7:17057
Pandey SN, Vishal V, Chaudhuri A (2018) Geothermal reservoir modeling in a coupled thermo-hydro-mechanical-chemical approach: a review. Earth-Sci Rev 185:1157–1169
Phuoc TX, Massoudi M, Wang P, McKoy ML (2019) Heat losses associated with the upward flow of air, water, CO_2 in geothermal production wells. Int J Heat Mass Transf 132:249–258
Rathnaweera TD, Wu W, Ji Y, Gamage RP (2020) Understanding injection-induced seismicity in enhanced geothermal systems: from the coupled thermo-hydro-mechanical-chemical process to anthropogenic earthquake prediction. Earth-Sci Rev 205:103182
Rossi E, Jamali S, Wittig V, Saar MO, von Rohr PR (2020) A combined thermo-mechanical drilling technology for deep geothermal and hard rock reservoirs. Geothermics 85:10177
Shu B, Wang Y, Zhu R, Liu L, Tan J, Dick J (2022) Experimental study of the heat transfer characteristics of single geothermal fracture at different reservoir temperature and in situ stress conditions. Appl Therm Eng 207:118195
Sun Z, Jiang C, Wang X, Lei Q, Jourde H (2020) Joint influence of in-situ stress and fracture network geometry on heat transfer in fractured geothermal reservoirs. Int J Heat Mass Transf 149:119216
Sun Z, Jiang C, Wang X, Zhou W, Lei Q (2021) Combined effects of thermal perturbation and in-situ stress on heat transfer in fractured geothermal reservoirs. Rock Mech Rock Eng 54:2165–2181
Talalay PG, Hong J (2021) Perspectives for development of ice drilling technology: continuation of the discussion. Ann Glaciol 62:143–156
Tritton DJ (1977) Physical fluid dynamics. Van Nostrand Reinhold Company Ltd
Wang J, Xu P, Li T, Zhu J (2017) Performance enhancement of organic Rankine cycle with two-stage evaporation using energy and exergy analyses. Geothermics 65:126–134
Xu F, Shi Y, Song X, Li G, Song Z, Li S (2023) The characteristics and laws of fracture damage in the long-term production process of high-temperature geothermal resources. Rock Mech Rock Eng 56:275–299
Zeng YC, Wu NY, Su Z, Wang XX, Hu J (2013) Numerical simulation of heat production potential from hot dry rock by water circulating through a novel single vertical fracture at Desert Peak geothermal field. Energy 63:268–282
Zhang L, He J, Wang H, Cen X (2022) Study on heat extraction characteristics in a rock fracture for the application of enhanced geothermal systems. Geothermics 106:102563
Zhao Y, Liu L, Wen D, Zhang B, Zhang X, Huan C, Wang M, Wang X (2022) Experimental study of horizontal ground heat exchangers embedded in the backfilled mine stopes. Geothermics 100:102344